Acta Materialia 132 (2017) 49–56

Contents lists available at ScienceDirect

Acta Materialia

journal homepage: www.elsevier.com/locate/actamat

Full length article

Pseudoelasticity and shape memory effects in cylindrical FCC metal nanowires

Reza Rezaei [a], Chuang Deng [b, *]

[a] Faculty of Mechanical Engineering, Shahrood University of Technology, Shahrood, 3619995161, Iran
[b] Department of Mechanical Engineering, University of Manitoba, 15 Gillson Street, Winnipeg, MB, R3T 5V6, Canada

ARTICLE INFO

Article history:
Received 20 February 2017
Received in revised form
23 March 2017
Accepted 18 April 2017
Available online 19 April 2017

Keywords:
Nanowire
Pseudoelasticity
Shape memory effect
Molecular dynamics

ABSTRACT

Molecular dynamics simulations are used to show strong pseudoelasticity and shape memory effects in a wide range of face-centered cubic metal nanowires with cylindrical shape, while similar effects have only been previously reported in face-centered metal nanowires with a unique geometry, i.e., by crystal reorientation from ⟨0 0 1⟩/{1 0 0} with a square cross section to ⟨1 1 0⟩/{1 1 1} with a rhombic cross section. The more generalized pseudoelasticity and shape memory effects reported in this work are enabled via a simple yet experimentally practical approach by tilting the nanowire axis away from the perfect ⟨0 0 1⟩ or ⟨1 1 0⟩ orientation such that the symmetry is broken in those nanowires and only one slip system is activated during the uniaxial loading. It is shown that while no pseudoelasticity and shape memory effects are found in ⟨1 1 0⟩ or ⟨0 0 1⟩ oriented cylindrical nanowires, full recovery up to ~50% tensile (or ~ 30% compressive) strain can be achieved in cylindrical nanowires whose axis are tilted as small as 2° (or 4°) away from ⟨1 1 0⟩ (or ⟨0 0 1⟩). This finding could open up new opportunities for synthesizing shape-memory metal nanowires for vibration damping and mechanical energy storage applications at low cost.

1. Introduction

Pseudoelasticity and shape memory effects through crystal reorientation in single-crystalline face-centered cubic (FCC) and body-centered cubic (BCC) metallic nanowires (NWs) have attracted dramatic attention of the materials community in the past decade [1–11]. In particular, the pseudoelastic behavior in ⟨1 1 0⟩/{1 1 1} FCC NWs with a rhombic cross section that was first predicted based on atomistic simulations has been recently confirmed by in-situ nanomechanical experiments. The pseudoelasticity or superplastic deformation in ⟨1 1 0⟩/{1 1 1} FCC NWs, for example, occurs through the nucleation and propagation of coherent twin boundaries upon tensile loading which reorients the NWs to ⟨0 0 1⟩/{1 0 0} with a square cross section. Atomistic simulations have also shown that such transformation is reversible exhibiting recoverable high pseudoelastic strain and shape memory effects, although experimentally it is impractical to compress a NW with high aspect ratio [2,3,5,11,12]. Moreover, as shown from atomistic simulations, temperature can also drive the crystal-reorientation-based phase transformation in the above-mentioned special FCC nanowires, which is similar to conventional shape memory effects in alloys through martensitic transformation [4,5,7,13].

Although these special NWs, e.g., Au ⟨1 1 0⟩/{1 1 1} NWs with rhombic cross section, have been successfully synthesized, they were based on a vapor transport method which requires a vacuum environment and high temperature of 1100 °C [14]. In contrast, there are some more economical and flexible methods to synthesize metal NWs such as electrodeposition [15]. In particular, template-assisted electrodeposition is a widely-used technique to synthesize cylindrical metal NWs whose microstructure can be easily controlled, e.g., single crystalline, nanocrystalline, or bamboo-structure with coherent twin boundaries, by varying the deposition voltage [16–18]. Furthermore, Burek and Greer [19] have developed a fabrication procedure of electron beam lithography and electroplating to synthesize metallic nanopillars into a prescribed template. It has been shown that with this technique one-dimensional cylindrical nanopillars with tilted (slanted) twins can be synthesized by controlling the relative angle between the electro-plates during the electrodeposition process. Recently, it has been proven by MD simulations [1] that cylindrical FCC metal NWs with tilted twin boundaries show strong pseudoelasticity and

* Corresponding author.
E-mail address: Chuang.Deng@umanitoba.ca (C. Deng).

http://dx.doi.org/10.1016/j.actamat.2017.04.039
1359-6454/

shape memory effects due to easy twinning and detwinning in those NWs under loading and reverse loading, respectively, which have an axial orientation different from the normal ⟨1 1 1⟩, ⟨1 1 0⟩, or ⟨0 0 1⟩ directions. It is therefore suspected that single crystalline NWs with tilted axis away from the ⟨1 1 0⟩ or ⟨0 0 1⟩ directions can also be synthesized by controlling both the applied voltage and the relative angle between the electrodes by using various electrodeposition methods, which may open ways to synthesize cylindrical single crystalline FCC metal NWs with strong pseudoelasticity and shape-memory effects.

In this work, we report a set of numerically constructed cylindrical FCC NWs with varying crystalline orientations exhibiting strong pseudoelasticity and shape memory effects with extremely high recoverable plastic strains. Twin boundary nucleation and propagation, which are responsible for the superplastic deformation previously reported only for ⟨1 1 0⟩/{1 1 1} and ⟨1 0 0⟩/{1 0 0} FCC NWs with rhombic and square cross sections, are also found to dominate the deformation in the tilted cylindrical FCC NWs with a wide range of axial orientations that are different from the normal axial directions ⟨1 1 0⟩ or ⟨0 0 1⟩.

2. Methodology

To represent the atomic interactions between the metallic atoms of the FCC metal NW specimens, embedded-atom method (EAM) potential was utilized for the metals Au [20], Ag [21], Al [22,23], Ni [24] and Cu [25]. As shown in Fig. 1(a) the NW with cylindrical structure is carved from a bulk material in a way that its axis forms an angle, θ, with the crystalline orientation ⟨1 1 0⟩. The angle falls into the closed interval [0, 90]. The endpoints correspond to the crystalline orientation ⟨1 1 0⟩ and ⟨0 0 1⟩, respectively. The NWs considered in this study are classified into two distinct sets in terms of the angle value. In the first set (denoted as Group I) the angle is less than 45°. It is composed of seven NWs which correspond to the crystalline orientations <1 1 0>, ⟨20 20 1⟩, ⟨10 10 1⟩, ⟨5 5 1⟩, ⟨5 5 2⟩, ⟨2 2 1⟩, and ⟨1 1 1⟩, respectively, as shown in Fig. 1(b). For the second set (Group II) the angle is larger than 45° (closer to ⟨0 0 1⟩ than ⟨1 1 0⟩). There are six NWs in Group II corresponding to the axial directions along ⟨1 1 2⟩, ⟨1 1 4⟩, ⟨1 1 5⟩, ⟨1 1 10⟩, ⟨1 1 20⟩, and ⟨0 0 1⟩, respectively, as shown in Fig. 1(b).

Periodic boundary conditions were applied along the NW axis z in all MD simulations. The lengths of the NW specimens varied from 35 to 40 nm depending on the axial orientation while their diameters were fixed at 9.8 nm. The specimens were equilibrated at 300 K for 100 ps under zero pressure with an isothermal-isobaric (NPT) ensemble. They were then stretched or compressed, respectively, for Group I and Group II, at 300 K with a constant engineering strain rate of 10^8 s^{-1} under a canonical (NVT) ensemble. The MD simulation software LAMMPS (Large-scale Atomic/Molecular Massively Parallel Simulator) was employed to perform all the simulations [26]. The stress was calculated based on the Virial theorem [27] and the visualization of atomic configurations was accomplished in OVITO [28] with common neighbor analysis [29].

3. Results and discussion

3.1. Deformation in ⟨1 1 0⟩ and ⟨0 0 1⟩ oriented cylindrical Au NWs

For comparison purposes, the deformation in ⟨1 1 0⟩ and ⟨0 0 1⟩ oriented cylindrical Au NWs under uniaxial tension and compression were first simulated respectively. Fig. 2(a) shows the stress-strain curve of the ⟨1 1 0⟩-oriented Au cylindrical NW under tensile loading. Its corresponding deformation mechanism is illustrated at the snapshot insets of the figure at different time steps of the applied strains. It is seen that the NW was first deformed elastically until the maximum tensile stress (~3.0 GPa at strain ~0.0485) was reached. It then experienced yielding because of the nucleation of stacking faults which quickly transformed into twin boundaries, as shown by the snapshot at strain 0.05 in Fig. 2(a). This is consistent with previous atomistic simulations and in-situ tensile experiments of ⟨1 1 0⟩/{1 1 1} Au NWs [2,10,12]. It is important to note that, however, two sets of slip system were activated in the cylindrical Au NWs studied here, which have the same Schmid factor respective to the ⟨1 1 0⟩ loading direction due to the symmetry. In contrast, only one set of slip system has been observed in previous atomistic simulations and experiments in ⟨1 1 0⟩/{1 1 1} FCC metal NWs under tensile loading. It may be due to the fact that in ⟨1 1 0⟩/{1 1 1} FCC metal NWs with rhombic cross section, the stress required to nucleate a stacking fault and twin boundaries from the {1 1 1} surface facets, which is known to have the lowest surface energy in FCC metals, is dramatically higher than that needed for twin boundary propagation. Therefore, twin boundary propagation will dominate the continuing deformation in ⟨1 1 0⟩/{1

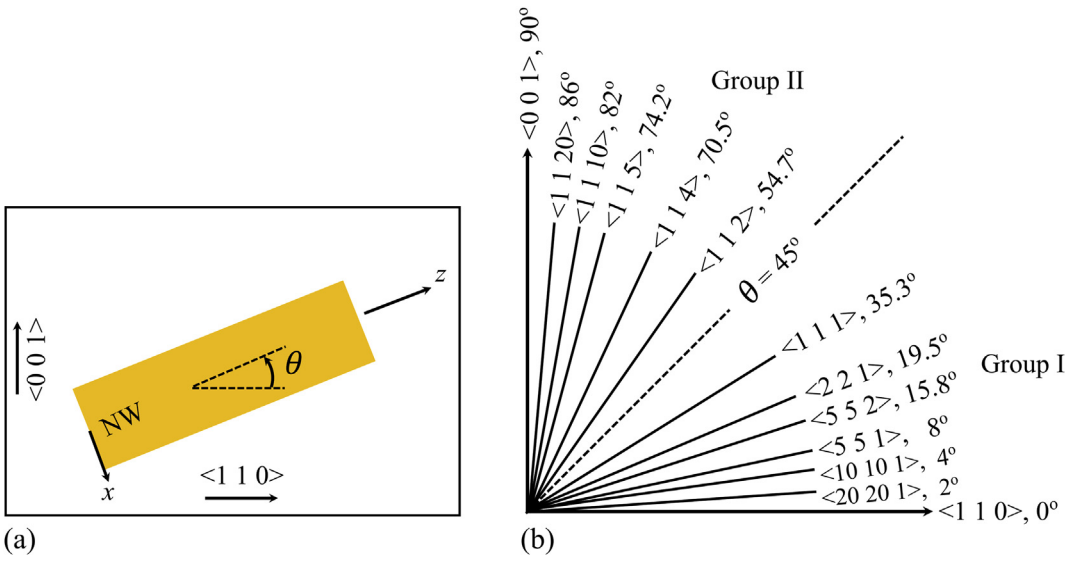

Fig. 1. Schematic of (a) a cylindrical NW carved from a bulk metal and (b) its axial orientation with respect to the crystalline directions ⟨1 1 0⟩ and ⟨0 0 1⟩.